Biochimica et Biophysica Acta 1808 (2011) 1661–1672

Contents lists available at ScienceDirect

Biochimica et Biophysica Acta

journal homepage: www.elsevier.com/locate/bbamem

Interactions between selected photosensitizers and model membranes: an NMR classification

Mattia Marzorati *, Peter Bigler, Martina Vermathen

Department of Chemistry and Biochemistry, University of Bern, Freiestrasse 3, CH-3012 Bern, Switzerland

ARTICLE INFO

Article history:
Received 1 October 2010
Received in revised form 21 January 2011
Accepted 11 February 2011
Available online 18 February 2011

Keywords:
NMR spectroscopy
Phospholipid bilayer
Membrane distribution
PS-membrane interaction
Chlorin
Porphyrin

ABSTRACT

Membrane interactions of porphyrinic photosensitizers (PSs) are known to play a crucial role for PS efficiency in photodynamic therapy (PDT). In the current paper, the interactions between 15 different porphyrinic PSs with various hydrophilic/lipophilic properties and phospholipid bilayers were probed by NMR spectroscopy. Unilamellar vesicles consisting of dioleoyl-phosphatidyl-choline (DOPC) were used as membrane models. PS-membrane interactions were deduced from analysis of the main DOPC ^{1}H-NMR resonances (choline and lipid chain signals). Initial membrane adsorption of the PSs was indicated by induced changes to the DOPC choline signal, i.e. a split into inner and outer choline peaks. Based on this parameter, the PSs could be classified into two groups, Type-A PSs causing a split and the Type-B PSs causing no split. A further classification into two subgroups each, A1, A2 and B1, B2 was based on the observed time-dependent changes of the main DOPC NMR signals following initial PS adsorption. Four different time-correlated patterns were found indicating different levels and rates of PS penetration into the hydrophobic membrane interior. The type of interaction was mainly affected by the amphiphilicity and the overall lipophilicity of the applied PS structures. In conclusion, the NMR data provided valuable structural and dynamic insights into the PS-membrane interactions which allow deriving the structural constraints for high membrane affinity and high membrane penetration of a given PS.

1. Introduction

Photosensitizers (PSs) are a class of compounds which performs an important role in photodynamic therapy (PDT). PDT is a widely accepted method for treatment of several diseases (mainly different types of cancer), and is used in medical fields like oncology and dermatology [1,2]. The mechanism behind this method is the photochemical reaction of the PS with oxygen which leads to the formation of highly oxidative species (mainly singlet oxygen, $^1O_2$) which trigger a sequence of oxidation reactions finally reaching cell death. This treatment is highly selective, because the tissue damage is achieved only if three components (PS, oxygen and light) are combined [3,4].

More recently, PSs are also used in photochemical internalization (PCI), in combination with "normal" drugs. PCI is a new approach based on the release of active molecules from endocytosed vesicles after photodynamic break-down of the irradiated vesicle [5]. Lately it has been reported that PCI improves the biological activity of several active macromolecules [6].

An ideal PS should have several features [7]: minimal dark toxicity, preferential uptake and/or retention by tissues of interest, high quantum yield for the generation of singlet oxygen ($^1O_2$), strong absorbance with a high extinction coefficient in the 600–900 nm range where penetration of light into tissue is optimal, rapid excretion leading to low systemic toxicity, low aggregation tendency and chemical properties conducive to efficient drug administration.

Chemical research continues to search novel PSs with improved combinations of chemical, photophysical and biological properties. Up to now, hundreds of different PSs are known [8]. Except for the common porphyrin or chlorin skeleton-based core, PSs can have different chemical structures. Important differences are the presence (or absence) of a metal ion [9], the presence of polar or unpolar lateral substituents [10] and the presence of anionic or cationic lateral side chains [11]. PS properties like solubility, aggregation tendencies and singlet oxygen yield are strictly related to the chemical structure. Therefore, there is currently great ongoing interest in understanding which molecular design of a PS is favorable for PCI and PDT [12]. In particular, it has been demonstrated that PSs with amphiphilic

Abbreviations: PSs, photosensitizers; PDT, photodynamic therapy; PCI, photochemical internalization; DOPC, dioleoyl-phosphatidyl-choline; CE, chlorin e6; RG7, rhodin G7; CEMED, chlorin e6 monoethylene diamine monoamide; m-CEMED, mesochlorin e6 monoethylene diamine amide; MACE, mono-L-aspartyl-chlorin e6; Arg-CE, arginine amide of chlorin e6; Tyr-CE, monotyrosine amide of chlorin e6; HPIX, hematoporphyrin IX; DPIX-DSME, deuteroporphyrin IX 2,4-disulfonic acid dimethyl ester; CPIII, coproporphyrin III; DPIX-DS, deuteroporphyrin IX 2,4-disulfonic acid; TCPhP, 5,10,15,20-Tetrakis-(4-carboxyphenyl)-21,23H-porphyrin; TSPhP, 5,10,15,20-Tetrakis (4-sulfonatophenyl)-21,23H-porphyrin; TMPyP, 5,10,15,20-Tetrakis-(N-methyl-4-pyridyl)-21,23H-porphyrin; THPhP, 5,10,15,20-Tetrakis-(3-hydroxyphenyl)-21,23H-porphyrin; PL, phospholipid; PBS, phosphate buffered saline

* Corresponding author. Tel.: +41 316314377, fax: +41 316313424.
E-mail address: mattia.marzorati@ioc.unibe.ch (M. Marzorati).

0005-2736/$ – see front matter © 2011 Elsevier B.V. All rights reserved.
doi:10.1016/j.bbamem.2011.02.011

properties are the most efficient in photochemical internalization of functional genes complexed to polylysine [13]. Amphiphilic PSs were localized mainly in the membrane of the endocytic vesicles, while ionic PSs remained mainly in the matrix and therefore were found to be less active toward membrane damage. Another study [14] has revealed that when incorporated in liposomes, apolar PSs showed better efficacy in terms of lipid peroxidation than the amphiphilic ones. On the other hand, the photoinduced permeation (process that takes place in PCI) of the same liposomes was higher when amphiphilic PSs were involved. These results demonstrate that amphiphilicity seems to be an important characteristic that a PS suitable for PCI should have. In a different work the in vitro effects of a series of dihydroxychlorins with different degree of amphiphilicity have been studied [15]. The aim of this study was to better understand the influence of amphiphilicity on intracellular uptake, subcellular localization and photosensitizing activity of some PSs. The results have shown that an increased amphiphilicity of the sensitizer molecules is correlated with an increased sensitizer uptake and an increased PDT efficiency.

Besides the chemical structure of the PSs, there is currently also great interest in the development of efficient and specific carrier delivery platforms for PDT [16] as, for example, PS-polymer conjugates [17] and PS-fullerene adducts [18].

Processes involved in PDT comprise several steps: first, the PS is injected into the blood stream, second, the PS binds to the blood vessel wall, and third, the PS penetrates the wall and diffuses into the extracellular medium of the tissue and finally penetrates into the tumor cells and locates in organelles. Owing to these processes, conditions like pH and potential protein-binding can vary a lot [19]. Considering also that different PSs have different pharmaco-kinetic and distribution properties, it is easy to understand that there are so many variables involved in the complete process that finding a perfect PS is quite a complex aim [20]. Because of that, effective photosensitizers are often discovered by "trial and error" procedures. As the cellular response to PDT is strictly related to the subcellular localization of the PS, and as the vesicle membrane distribution of PSs is a key step in PCI, the behavior of PSs towards the membrane is currently a very attractive research topic [21]. Despite numerous publications around this topic, there is still no clear knowledge of all the mechanisms involved. Therefore, there is great ongoing interest in understanding the factors modulating the interactions between photosensitizers and membranes, and several studies in this field have been carried out, mainly involving fluorescence spectroscopy [22].

We previously demonstrated that NMR can be an efficient method to understand certain processes involved in the interactions between PSs and model membranes [23,24]. Up to now several NMR studies by other groups have been applied to study the transport and the dynamics of various non-porphyrinic compounds across lipid bilayer membranes [25–27].

In this work we studied the interaction between a series of commercially available PSs and model membranes probed by NMR spectroscopy. The main aim was to find correlations between molecular structure of the PS and its interactions with membranes.

As membrane models, unilamellar vesicles consisting of dioleoyl-phosphatidyl-choline (DOPC) were used. Several chlorin and porphyrin skeleton-based PSs having different chemical properties were employed (Fig. 1):

Chlorin e6 (CE (1)), Rhodin G7 (RG7 (2)), Chlorin e6 monoethylene diamine monoamide (CEMED (3)), Mesochlorin e6 monoethylene diamine amide (m-CEMED (4)), Mono-L-Aspartyl-Chlorin e6 (MACE (5)), Arginine amide of chlorin e6 (Arg-CE (6)), Monotyrosine amide of chlorin e6 (Tyr-CE (7)), Hematoporphyrin IX (HPIX (8)), Deuteroporphyrin IX 2,4-disulfonic acid dimethyl ester (DPIX-DSME (9)), Coproporphyrin III (CPIII (10)), Deuteroporphyrin IX 2,4-disulfonic acid (DPIX-DS (11)), 5,10,15,20-Tetrakis-(4-carboxyphenyl)-21,23H-porphyrin (TCPhP (12)), 5,10,15,20-Tetrakis(4-sulfonatophenyl)-21,23H-porphyrin (TSPhP (13)), 5,10,15,20-Tetrakis-(N-methyl-4-pyridyl)-21,23H-porphyrin (TMPyP (14)) and 5,10,15,20-Tetrakis-(3-hydroxyphenyl)-21,23H-porphyrin (THPhP (15)).

Analysis of the ^{1}H-NMR phospholipid (PL)-vesicle resonances permits to understand the membrane affinity and localization of the PS, and is a useful tool to obtain an approximate model of the diffusion of PSs within the bilayer.

The method takes advantage of the PS ring current effect inducing major shift changes to the ^{1}H-NMR signals of PL-molecules in spatial proximity. This shifting effect is – within certain limits – proportional to the amount of PS close to the PL molecules. Analyzing these induced chemical shift changes enables to obtain approximate information on the adsorption, the time-dependent movement and on the penetration of PSs into the lipid bilayer.

In this paper, we propose a classification of the investigated PSs with respect to their interactions with model membranes. Two main groups (called Model-A and Model-B) can be defined based on the initial and fast adsorption of the PS to the outer membrane layer. Each group can be subsequently divided into two further sub-groups (called Model-A1, Model-A2, Model-B1, Model-B2) based on the slower diffusion of the PS into and within the two membrane layers. A correlation between PS structure and type of membrane interaction is suggested.

2. Materials and methods

2.1. Materials

18:1 PC (cis) 1, 2-dioleoyl-sn-glycero-3-phosphocholine (DOPC) was purchased from Avanti Polar Lipids Inc. Deuteroporphyrin IX 2,4-disulfonic acid dihydrochloride (DPIX-DS), Coproporphyrin III dihydrochloride (CPIII), Chlorin e6 (CE), Mono-L-Aspartyl-Chlorin e6 tetrasodium salt (MACE, Npe6), Rhodin G7 sodium salt (RG7), Hematoporphyrin IX dihydrochloride (HPIX), Deuteroporphyrin IX 2,4-disulfonic acid dimethyl ester disodium salt (DPIX-DSME), Monotyrosine amide of chlorin e6 trisodium salt (Tyr-CE), Arginine amide of chlorin e6 trisodium salt (Arg-CE), Chlorin e6 monoethylene diamine monoamide disodium salt (CEMED) and Mesochlorin e6 monoethylene diamine amide disodium salt (m-CEMED) were purchased from Frontier Scientific. 5,10,15,20-Tetrakis-(3-hydroxyphenyl)-21,23H-porphyrin (THPhP), 5,10,15,20-Tetrakis-(4-carboxyphenyl)-21,23H-porphyrin (TCPhP), 5,10,15,20-Tetrakis(4-sulfonatophenyl)-21,23H-porphyrin (TSPhP) and 5,10,15,20-Tetrakis-(N-methyl-4-pyridyl)-21,23H-porphyrin tetratosylate were purchased from Porphyrin Systems GbR. The 4 tosylate counterions in 5,10,15,20-Tetrakis-(N-methyl-4-pyridyl)-21,23H-porphyrin tetratosylate were replaced by chloride ions using an ionic exchange resin in order to obtain 5,10,15,20-Tetrakis-(N-methyl-4-pyridyl)-21,23H-porphyrin tetrachloride (TMPyP). MeOH, CH_2Cl_2 and $CHCl_3$ were purchased from Sigma-Aldrich. Deuterated water (D_2O, D 99.9%) and DMSO-d6 were obtained from Cambridge Isotopes Laboratories, Inc. Trimethyl-silyl-3-propionic acid-d4 sodium salt (TMSP-d4, D 98%), obtained from Euriso-Top, was used as internal ^{1}H-NMR reference. All chemicals and solvents were used without further purification. PS stock solutions were freshly prepared in DMSO-d6 at a concentration of 15 mM. Phosphate buffered saline (PBS) solution of pH-values of 6.9 was prepared by mixing different aliquots of 50 mM solutions of KH_2PO_4 and Na_2HPO_4 (both Sigma-Aldrich) in D_2O containing 0.9% NaCl.

2.2. Solubility of selected PS compounds

The water solubility of the applied PS for our study was quite heterogeneous: some were water soluble, others were water soluble after the formation of the salt and some were water insoluble. Therefore, we decided to prepare all PS stock solutions in DMSO (good solvent for all PSs) to keep the experimental conditions constant. A

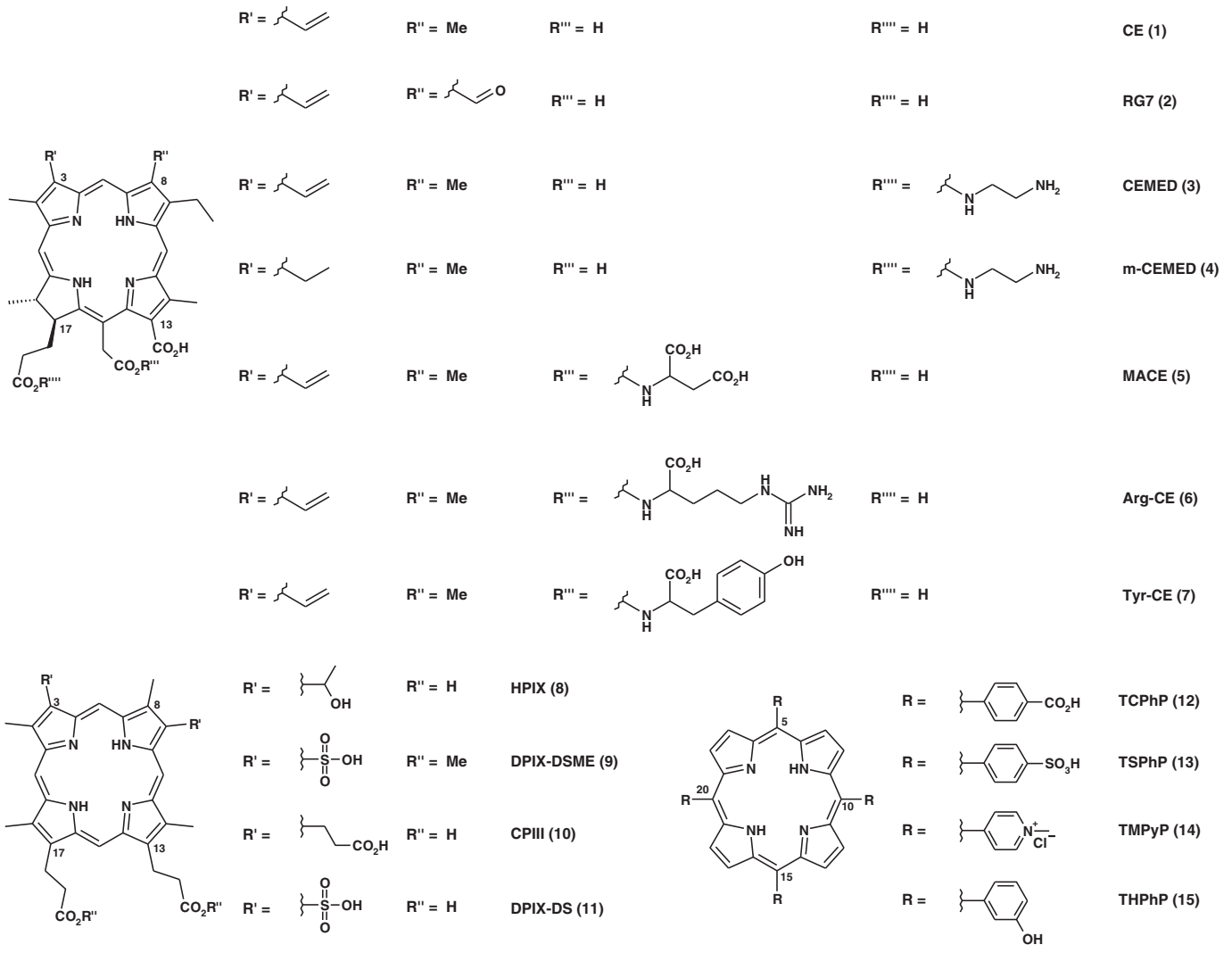

Fig. 1. Chemical structures of the investigated compounds.

blank experiment has been performed with a water soluble PS (MACE) using both, a DMSO and a water stock solution, confirming that the small amount of DMSO added to the vesicle solutions does not affect the results. Moreover, DMSO is a well known delivery mode usually applied with in vitro studies to several water insoluble PSs [28].

2.3. Vesicle preparation

Unilamellar DOPC vesicle (50–60 nm in diameter) solutions (10 mM DOPC) in PBS at pH 6.9 were prepared by the extrusion method as previously described [23]. A slightly acidic pH was used as the extracellular pH in tumors is typically in the range of 6.5–6.9 [29].

2.4. Vesicle loading with PSs

480 μl of 10 mM DOPC-solution in PBS were transferred to 5 mm NMR tubes (Wilmad) and aliquots of PS stock solutions were added and mixed in the NMR tube to yield the desired molar ratio of PS/DOPC (8 μl for 0.025 molar ratio, and 32 μl for 0.1 molar ratio). Prior to each series of NMR measurements the pH of each sample was measured directly in the NMR tube using a pH-electrode designed for NMR tubes (Spintrode 180×3 mm, Hamilton). The time between mixing of the PS stock solution with DOPC vesicles and the first NMR acquisition ("dead time") was about 8 minutes due to several preparation steps (e.g. pH measurement, matching and tuning of the NMR probe, locking-, and shimming procedure). Stability of these PS-vesicle systems during the course of the experiments has been previously evaluated by NMR and DLS measurements [23].

To obtain a sample of 10 mM DOPC vesicles preloaded with CE, defined amounts of DOPC and CE were dissolved in MeOH/CH_2Cl_2 (1:1). After solvent removal, the DOPC/CE mixture was hydrated with PBS, vortexed, and then submitted to freeze–thaw cycles and extrusion.

2.5. Nuclear magnetic resonance (NMR) spectroscopy

The NMR experiments were performed on a Bruker Avance II spectrometer operating at a resonance frequency of 500.13 MHz for ^{1}H nuclei. The instrument is equipped with a 5 mm dual probe (BBI) for inverse detection with a z-gradient coil. All experiments were carried out at room temperature (298 K).

^{1}H-NMR spectroscopy: For time-dependent ^{1}H-NMR measurements, a coaxial inner tube (WGS-5BL Wilmad) containing 60 μL of 1 mM TMSP in D_2O was inserted into each NMR sample tube as internal reference. The ^{1}H-NMR spectra were recorded using a 1D NOESY presaturation sequence with spoil gradients for residual water suppression ("noesygppr1d" from the Bruker pulse-program library). Typically 16 transients, a spectral width of 7352.9 Hz, a data size of 64 K points, an acquisition time of 4.46 s, and a relaxation delay of 6 s were used to acquire the ^{1}H-NMR spectra. The co-added free

induction decays (FIDs) were exponentially weighted with a line broadening factor of 1.0 Hz, Fourier-transformed, and phase corrected to obtain the ^{1}H-NMR spectra.

2.6. Analysis of time-dependent PS distribution across the bilayer

Time-dependent ^{1}H-NMR spectra of DOPC-vesicle solutions were recorded after the addition of the PS, in molar ratios of 0.025 and 0.1 (PS/DOPC). The ^{1}H chemical shifts $\delta(t)$ of the DOPC inner -$N^+(CH_3)$, -$(CH_2)_n$-, and ω-CH_3 signals at time t after mixing were normalized to their initial values of $\delta_0(t=0)$ (i.e., the chemical shift measured directly after mixing):

$$\delta_n(t) = \delta(t) / \delta_0(t = 0)$$

These $\delta_n(t)$ values were plotted as a function of time for each compound. To derive the rate constants for PS distribution across the membrane, a model was chosen for data fitting comprising three components: two exponentials and one sigmoidal component [24]. The components were included in the fitting function used to calculate the normalized chemical shift $\delta_n(t)$:

$$\delta_n(t) = A\left(e^{(-t/t_1)} + We^{(-t/t_2)}\right) + \frac{S_1 - S_2}{1 + e^{(t-t_s)/t_s}} + S_2$$

The fitting was applied simultaneously to all three DOPC resonances with shared parameters for the time constants (t_1, t_2, t_3 and t_s) and the weighting factor W. The independent parameters (A, S_1, and S_2) account for differences in magnitude of temporal chemical shift changes for all three resonances. In the major part of the cases a simplified fitting function was used, using only one or two components. Fitting procedures were carried out using Origin version 5.0 (Microcal Software, Inc.). The Levenberg–Marquardt algorithm was applied to minimize the sum of squares. The number of iteration steps was determined by the convergence criterion.

3. Results and discussion

3.1. Overview

3.1.1. Sensors

^{1}H-NMR is a valuable and useful method for the study of the dynamics involved in a PS-vesicle system. The ^{1}H-NMR spectrum of DOPC vesicles in PBS is shown in Fig. 2A. The most prominent peak in the DOPC spectrum derives from the choline methyl protons, which is a sharp singlet at 3.27 ppm. In unilamellar DOPC bilayer vesicles, there are two different choline moieties: one belongs to the inner layer, the other to the outer layer. In the ^{1}H-NMR spectrum of free DOPC vesicles, the choline resonance at 3.27 ppm is the sum of the outer and inner choline signals, which have the same linewidth and chemical shift. The other two peaks of main interest originate from the lipid chain methylene protons (1.33 ppm) and the terminal ω-methyl group (0.92 ppm). The induced chemical shift changes and temporal evolution of these resonances are of particular importance for characterizing the PS-membrane interaction and allow the investigated PSs to be classified.

For the first level classification (Model-A and Model-B) we have focused on the choline resonance, in particular on the presence/absence of a split of the choline signal immediately after mixing the PS and DOPC solutions. The split consists of two clearly resolved singlets, one slightly upfield shifted (at ~3 ppm) and one not shifted (at 3.27 ppm, as in the free vesicle). The shifted peak can be assigned to the outer layer of the vesicles, with its choline methyl protons interacting with the PS. On the other hand, the non-shifted peak can be assigned to the inner layer, where initially no PS is present (Fig. 2B). The width of the split is an indication of the amount and interaction strength of PS bound to the outer layer of the vesicle.

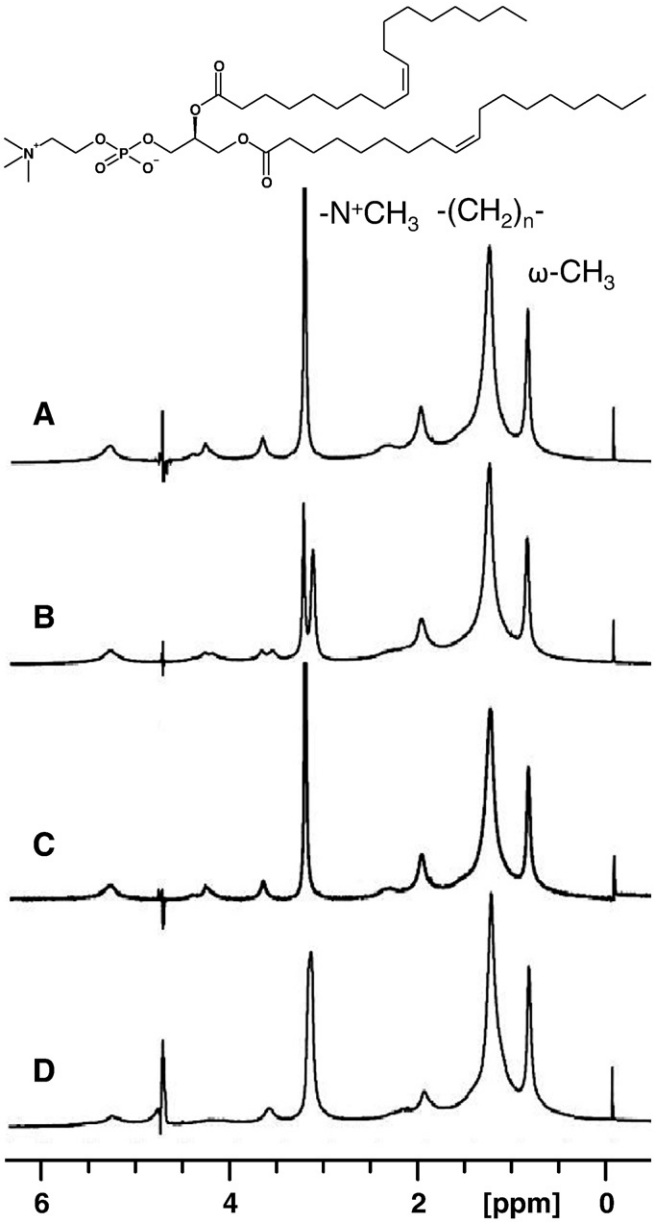

Fig. 2. Structure and ^{1}H-NMR spectra of 1,2-dioleoyl-sn-glycero-3-phosphocholine (DOPC) vesicles (A), DOPC vesicles after external addition of CE (Type-A PS) (B), DOPC vesicles after external addition of TSPhP (Type-B PS) (C) and DOPC vesicles preloaded with CE (D). All spectra were recorded in PBS (D_2O, pH 7) at a DOPC concentration of 10 mM and molar ratios of PS/DOPC of 0.1 (B–D).

The intra-membrane distribution of the PS can be followed by time-dependent chemical shift changes from their initial (δ_0) towards equilibrium (δ_e) values. The second level classification (Model-A1, -A2, -B1 and -B2) was based on the following criteria: 1) The temporal evolution of the chemical shift of the inner and outer choline signals between $t=0$ and equilibrium. The magnitude of chemical shift change is assumed to reflect an increase or decrease of PS at or close to the surface of the outer vesicle layer. 2) The equilibrium chemical shift values of the three main peaks originating from the internal part of the bilayer, i.e. the inner choline group —$N^+(CH_3)_3$, the lipid chain methylene groups —$(CH_2)_n$— and the terminal methyl group ω-CH_3.

In the course of the diffusion process a general decrease of the chemical shift of these resonances is detected which is attributed to an increase of embedded PS in the membrane. This decrease typically following either a mono- or bi-exponential decay is characterized by different rate constants and different equilibrium values depending

on the respective PS. Again, the magnitude of chemical shift change is assumed to reflect the PS proximity and concentration change close to the corresponding groups. Therefore these changes for the —$(CH_2)_n$— and ω-CH_3 resonances measured at equilibrium are a qualitative measure for the PS amount in the hydrophobic core of the bilayer system. Correspondingly the equilibrium value for the inner choline —$N^+(CH_3)_3$ resonance is a qualitative measure of PS amount close or at the internal surface of the vesicle.

3.1.2. Structure based PS classification

In this work a large group of commercial porphyrin and chlorin compounds has been studied (Fig. 1). These compounds have been chosen to cover a large variety of chemical structures showing different hydrophilic/lipophilic balances. Different allocations and characteristics of hydrophilic and lipophilic moieties within these molecules allow the main principles governing PS uptake by membranes to be recognized and understood. The PSs used in this work can be separated into two main groups, the asymmetric compounds with hydrophilic and lipophilic domains (compounds (1)–(9)) and compounds with polar and non-polar structural elements arranged more or less symmetrically (compounds (10)–(15)).

The group of asymmetric compounds may be divided into a subgroup of distinct amphiphilic PSs (compounds that contain two molecular moieties with pronounced hydrophilic and hydrophobic character respectively) and a subgroup of less distinct amphiphilic PSs (compounds with a less pronounced hydrophobic character due to polar structural elements in the hydrophobic moiety). The first subgroup includes the chlorins CE (1), RG7 (2), CEMED (3) m-CEMED (4), MACE (5), Arg-CE (6) and Tyr-CE (7), the second subgroup includes the two porphyrins HPIX (8) and DPIX-DSME (9).

The non-amphiphilic PSs may be divided into a subgroup with ionizable or ionic hydrophilic moieties, i.e. CPIII (10), DPIX-DS (11), TCPhP (12), TSPhP (13) and TMPyP (14), and a single compound with less pronounced hydrophilic moieties, i.e. THPhP (15).

For all types of porphyrins with ionizable structural elements (carboxylic or sulfonic groups) the hydrophilic character is expected to be pH dependent.

3.1.3. The membrane and the basic steps of PS-membrane interactions

A buffered small unilamellar vesicle (SUV) solution is composed of 4 different environments (Fig. 3, right): the external aqueous bulk solution, the outer vesicle layer, the inner layer and the entrapped aqueous volume. The two membrane layers are purely amphiphilic with a hydrophilic and a hydrophobic domain. The membrane bilayer with the distinct hydrophobic inner domain and the two hydrophilic surfaces exposed to the external and internal aqueous bulk respectively forms in some sense a bi-amphiphilic barrier for penetrating compounds such as PSs. From an experimental point of view, upon mixing the PS with the vesicles, two different periods of time should be taken into account.

The first encompasses the time between PS addition and the first recorded NMR spectrum (see Section 3.2). This period is characterized by a fast perturbation of the vesicle system due to PS adsorption to the vesicles outer surface (process I in Fig.3, left) and cannot be analyzed timely resolved by the NMR method. This adsorption is much faster than the subsequent intra-membrane distribution process. This fast adsorption mechanism will be characterized as "initial affinity." While for some PSs this "initial affinity" is high, it is rather low or not even present for others.

The second time period starts from the first acquired spectrum and ends at the equilibrium of the PS distribution process (see section 3.3 Second Phase). The second time period can be considered the main kinetic process. It encompasses the penetration and distribution of the PS from the outer to the inner membrane layer (process II in Fig.3, left). The last step (process III in Fig.3, left), the release of the PS into the inner volume, is neglected here, as has been done in previous kinetic studies [30], because the vesicle enclosed aqueous volume constitutes only a small fraction of the total aqueous bulk volume in diluted vesicle solutions.

The aim of this work is to find correlations between the chemical structure of the various PSs and their interactions with the model membrane on the basis of the PS classification outlined in chapter 3.1.2. A standardized common experimental procedure was applied to the PSs shown in Fig. 1 in order to compare the corresponding membrane interactions.

However, the study of this interaction is also affected by PS self-association in the external aqueous bulk solution. Even at very low concentration the selected PSs predominately self-associate in water and form aggregates as could be derived from the ^{1}H-NMR spectra. These aggregates can be small and water soluble but also very large leading to precipitation. While in water some ^{1}H-NMR signals are broadened due to aggregation, in DMSO usually sharp signals are observed throughout. Hence, it can be assumed that in DMSO PSs are mainly in monomeric form.

Ideally, PS-membrane interactions are studied with PS existing as monomers in the external bulk solution. However, spontaneous formation of supramolecular entities after addition of PS dissolved in DMSO to aqueous vesicle solutions is likely to occur as competitive process and complicates this study. This has to be taken into account when correlating PS structural properties with their membrane interaction behavior.

3.2. First Phase (I)

3.2.1. Experimental results

All PSs shown in Fig. 1 were each added to a solution of 10 mM DOPC SUV at two different molar ratios: PS/DOPC of 0.025 and 0.1. Immediately after mixing, a ^{1}H-NMR spectrum of the vesicle-PS mixture was recorded and the choline resonance was analyzed. As mentioned above, while in PS-free DOPC vesicles the choline ^{1}H-NMR signal

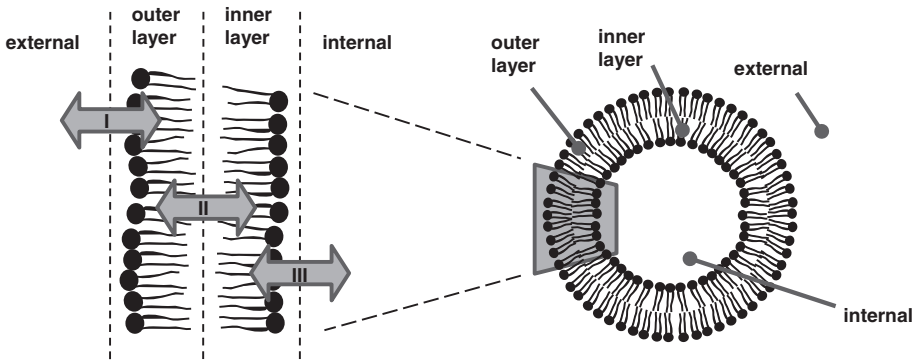

Fig. 3. Left: three equilibrium steps involved in the PS distribution process between the bilayer. Right: model membrane with the 4 environments.

Table 1
Classification of PS by initial affinity. For Type-A PSs, the width of the choline ^{1}H-NMR signal split is given for low and high molar ratio of PS/DOPC. n.a.: not applicable.

PS		Type	Split [Hz]	
			Molar ratio PS/DOPC	
			0.025	0.1
CE	**(1)**	A	49	135
RG7	**(2)**	A	27	74
CEMED	**(3)**	A	25	88
m-CEMED	**(4)**	A	30	102
MACE	**(5)**	A	62	141
Arg-CE	**(6)**	A	40	126
Tyr-CE	**(7)**	A	44	131
HPIX	**(8)**	A	22	55
DPIX-DSME	**(9)**	A	18	26
CPIII	**(10)**	B	n.a.	n.a.
DPIX-DS	**(11)**	B	n.a.	n.a.
TCPhP	**(12)**	B	n.a.	n.a.
TSPhP	**(13)**	B	n.a.	n.a.
TMPyP	**(14)**	B	n.a.	n.a.
THPhP	**(15)**	B	n.a.	n.a.

appears as a singlet, just after adding the PS solution, this resonance shows two different behaviors. As summarized in Table 1, some PSs generate a well resolved initial split of the choline signal, indicating immediate interaction and affinity with the outer membrane surface. Other PSs however do not induce any resolved split of the choline signal, indicating no measureable membrane interaction and affinity. The shift of the outer choline signal is attributed to the ring-current effect of nearby aromatic porphyrin. Table 1 summarizes the results related to this first phase of the PS-DOPC interactions. In case of a split choline resonance, the widths of the split (in Hz) observed for low and high PS concentration (0.025 and 01. PS/DOPC molar ratio) are reported.

PSs inducing an initial split of the choline signal are classified as Model-A and will be called "Type-A PSs". PSs inducing no initial split are classified as Model-B and will be called "Type-B PSs".

3.2.2. Interactions of the membrane surface with Type-A PSs (Model A)

The high initial membrane affinity of Type-A PSs for the outer membrane surface, as reflected by the initial choline signal split and the selective slight broadening of one of the choline signals (Fig. 2B), can most likely be attributed to their asymmetric and amphiphilic character as outlined in chapter 3.1.2. All these PSs (CE (**1**), RG7 **(2)**, CEMED **(3)**, m-CEMED **(4)**, MACE **(5)**, Arg-CE **(6)**, Tyr-CE **(7)**, HPIX **(8)**, DPIX-DSME **(9)**) bear two or more ionizable moieties (i.e. carboxylic or sulfonic groups) on the one, hydrophilic side of the structure, while they are rather non-polar on the other side. As the pH of the vesicle solution is in the neutral range (pH~7), all acidic groups (both carboxylic and sulfonic) in these PSs are mostly deprotonated. This anionic side of the molecule most likely causes electrostatic interactions with the cationic head of the PL leading to the electrostatically driven adsorption of PSs to the outer vesicle surface. The hydrophobic side seems to fold immediately into the outer membrane layer so that the outer PL head groups experience the porphyrin ring current causing the choline signal split.

Comparing the experiments carried out at low and high PS concentration, there is a clear difference in the magnitude of the induced split of the choline resonance for Type-A PSs (Table 1). At high concentration, the split values are clearly increased. Essentially, a higher amount of PS added to the vesicle solution also leads to a higher amount of PS embedded into the outer surface of the membrane thereby inducing a larger upfield shift of the outer choline resonance. However, the amount of PS adsorbed to the membrane approaches a limit as saturation of the outer layer is achieved. As shown in Fig. 4, with increasing amount of PS in the vesicle solution the split value increases and finally reaches a constant value.

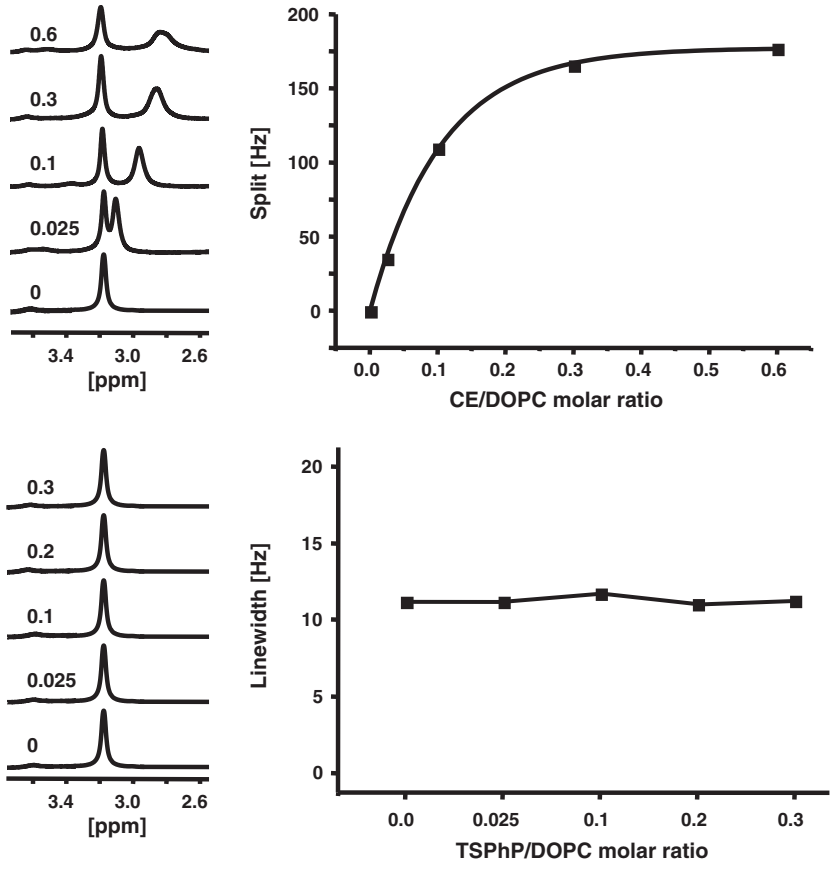

Fig. 4. Top: split choline signal at different concentrations of CE (Type-A PS). Bottom: choline signal and its corresponding linewidth at different concentrations of TSPhP (Type-B PS).

The initial amount of membrane bound PS depends on the total amount of PS added to the solution, but not exclusively. The data in Table 1 show that comparing same concentrations of PS, very different split values are observed for Type-A compounds, which must be attributed to the different structural properties. At both molar ratios (0.025 and 0.1), CE (1) and MACE (5) show the highest split values (49 and 62 Hz at 0.025 and 135 and 141 Hz at 0.1, respectively) while DPIX-DSME (9) and HPIX (8) show the lowest values (18 and 22 Hz at 0.025 and 26 and 55 Hz at 0.1, respectively).

The high values found for CE (1) and in particular for MACE (5) and hence their high membrane surface affinity are probably due to their strong amphiphilic character. The two compounds possess on one hand three and four (at pH 7 ionized) carboxylic moieties and on the other hand a distinct lipophilic molecular moiety. Electrostatic interactions among the corresponding polar domains and interactions among the corresponding lipophilic domains are most probably the main cause for the initial tight binding of PS in the outer surface of the PL-layer [31]. The low split values for HPIX (8) and especially for DPIX DSME (9) and hence their lower membrane surface affinity, may be attributed to their attenuated amphiphilic character. With only two ionized groups (—COO^- and —SO_3^- respectively), the hydrophilic character of the polar molecular moiety is less pronounced compared to CE (1) and MACE (5). On the other hand, the lipophilic character of the opposite site is weakened due to the presence of two slightly polar substituents (hydroxyl and ester groups, respectively). The very low split values measured for DPIX DSME (9) at both molar ratios could be due to the presence of the sulfonic acid instead of carboxylic acid side chains in this structure. Apparently, sulfonic acid groups show less interaction with the polar choline head of the PL, even if they are more acidic than carboxylic acid groups.

The residual Type-A PSs such as m-CEMED (4) or RG7 (2) show intermediate choline split values compared to CE (1) or MACE (5) and are assumed to be slightly less amphiphilic.

m-CEMED (4) is also highly lipophilic on one molecular side, but less hydrophilic due to only two (instead of three) ionizable groups in the other side. RG7 (2) on the other hand is highly hydrophilic on one molecular side, but less lipophilic due to a polar substituent in the other side.

3.2.3. Interactions of the membrane surface with Type-B PSs (Model B)

Compounds (10)–(15) were classified as Type-B PSs because in their presence no initially split choline signal was observed. The lack of initial split, shift or apparent signal broadening (with respect to the PS-free vesicles) of the choline signal (Fig. 2C) indicates low initial membrane affinity of Type-B PSs for the outer membrane surface and must be attributed to their symmetric and weak amphiphilic character as outlined in chapter 3.1.2. Thus, no PS seems to be present in the outer layer, or at least only at a very low amount, not enough to induce any spectral changes with the two surfaces remaining equivalent. However, the choline resonance can also appear as a singlet when the amount of PSs is nearly the same in both surfaces. This can be achieved with equal PS distribution in the two layers, either after equilibration of PS diffusion into the intact vesicles, or when preparing vesicles in the presence of porphyrins (PS-preloaded vesicles). In these cases the choline signal is slightly upfield shifted and broader as compared to the free vesicles due to the presence of PS now in both layers (Fig. 2D).

The "Type-B PSs" show no such shift and therefore no detectable immediate interactions with the model membrane (Table 1). Anchoring of the symmetric Type-B PSs in the outer membrane surface most likely is hindered for two reasons: 1. With ionic PSs such as CPIII (10), DPIXDS (11), TCPhP (12), TSPhP (13) and TMPyP (14), electrostatically driven adsorption may occur, but subsequent embedding for these PSs is hindered due to the lack of a cohesive lipophilic moiety. 2. With non-ionic PSs such as THPhP (15) on the other hand, embedding into the non-polar part of the outer layer might occur, but the first, electrostatically governed adsorption step is hindered. Hence, Type-B PSs all show low membrane surface affinity irrespective whether they are ionic or not.

The absence of the initial membrane surface affinity seems to be strictly related to the chemical structure of the PS and seems to be rather independent of the PS concentration. As shown in Fig. 4, for Type-B PSs, even at high PS/DOPC molar ratio (up to 0.3), no split of the choline resonance is observed. The linewidth of the choline peak remains constant for all PS concentrations applied (11–12 Hz, as in free vesicles). This is a clear indication that even at high PS concentration, there is not any fast measurable interaction with the DOPC vesicles. Self-association may rather be the preferred competing process for Type-B PSs, either taking place in the aqueous bulk or on the vesicle surface.

In conclusion, the data suggest that distinct molecular asymmetry with a hydrophilic and a lipophilic moiety, i.e. pronounced amphiphilicity is the basic prerequisite causing high affinity of a PS for the surface of the model membrane. Thus, both, hydrophilic and hydrophobic interactions can take place simultaneously favoring porphyrin anchorage at the membrane surface.

These conditions are not fulfilled by the symmetric porphyrins, which therefore don't show any initial affinity with the outer membrane layer.

3.3. Second phase (II)

3.3.1. Experimental results

Up to now we have only examined the initial interaction of the PS with the vesicle surface observed directly after mixing. During this "First phase" (Fig. 3, left: (I)), only the choline resonance undergoes changes if any. The other DOPC-vesicle peaks of interest, i.e. -$(CH_2)_n$- and ω-CH_3, do not show any alterations. This seems reasonable considering the thickness of the DOPC bilayer which is reported to be 3.8 nm [32] or about 5 nm including hydration water and distribution probabilities [33] and the average diameter of the porphyrin being about 13 Å [34]. Taking the distribution profile of the DOPC molecular groups along the bilayer normal into account [33], the porphyrin initially most likely resides in the interfacial membrane part which is characterized by a steep polarity gradient consisting of hydration water, the PL head-group region and the front part of the lipid chain.

Subsequently, a dynamic process, slow on the NMR time scale, takes place during the Second Phase (Fig. 3, left: (II)), which must be attributed to a slow PS uptake or distribution within the membrane. This is indicated by the time-dependent changes of the ^{1}H-NMR resonances of the inner vesicle protons, i.e. the —$(CH_2)_n$— and ω-CH_3 protons, but also of the choline protons of the inner vesicle surface.

To monitor the kinetic process of each PS-vesicle system, a series of ^{1}H spectra was recorded repeatedly until equilibrium was reached (typically ≥ 300 h), indicated by constant chemical shifts. According to the different membrane-uptake behaviors observed, a further classification into two subgroups, A1, A2, B1, and B2, is proposed and will be discussed below. For characterizing the second phase, we focused on the following experimental parameters: 1) The qualitative time evolution of the inner and outer choline resonances (Fig. 5) reflecting processes close to the two membrane surfaces. 2) The normalized equilibrium values δ_e/δ_0 of the —$(CH_2)_n$—, ω-CH_3 and the inner choline signals providing a measure for the total PS uptake and the PS distribution within the membrane reached at equilibrium (Figs. 6–8).

In Fig. 5, the temporal chemical shift evolution for the inner and outer choline resonances is displayed. The representative spectra (choline region) and the corresponding schematic plots show 4 different trends found for the two main types of porphyrins assigned as Model-A1, -A2, -B1 and -B2 respectively. Whereas the resonance of the inner choline undergoes a more or less pronounced upfield shift throughout, indicating an increasing amount of porphyrins in or close

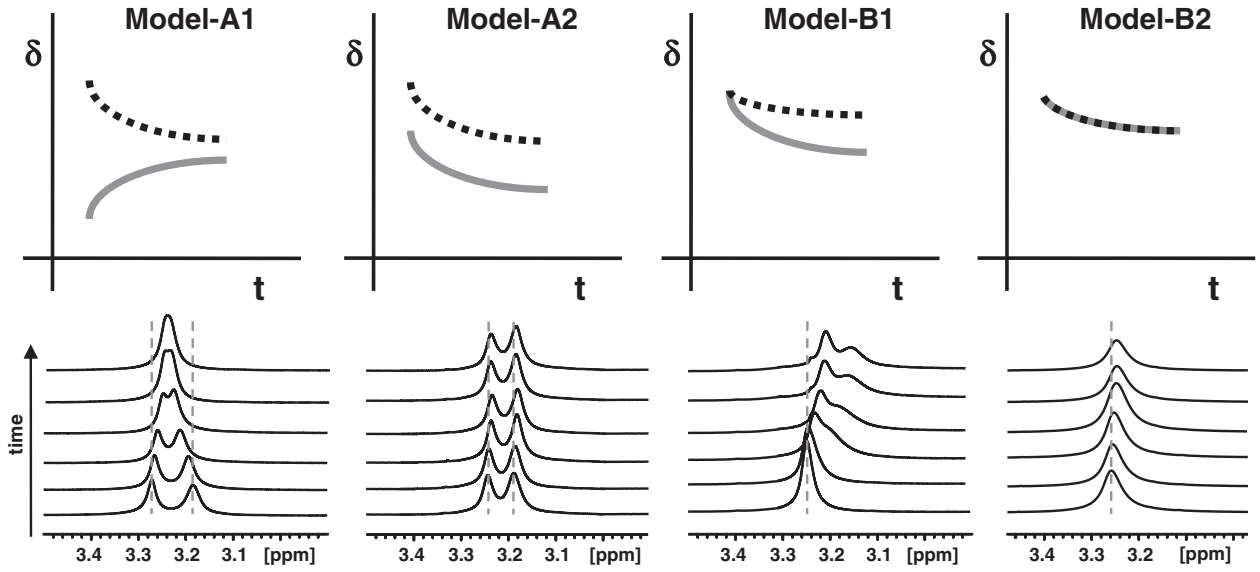

Fig. 5. Top: time-dependent inner (dashed black line) and outer (solid grey line) choline signal shift trends and their assigned classification into Model-A1, -A2, -B1, and -B2. Slopes are indicative. Bottom: ^{1}H-NMR spectra of DOPC -$N^+(CH_3)_3$ signals at various time points representative for the 4 models, after the addition of RG7, HPIX, THPhP and TMPyP to DOPC vesicles (molar ratio of PS/DOPC = 0.1).

to the inner membrane surface and hence PS uptake in general, different trends are visible for the resonance of the outer choline. For Model-A with initially split choline resonances, two trends are observed of the outer choline resonance, a downfield (Model-A1) or an upfield (Model-A2) shift, indicating a PS depletion or accumulation at the outer surface, respectively. For Model-B the resonance of the

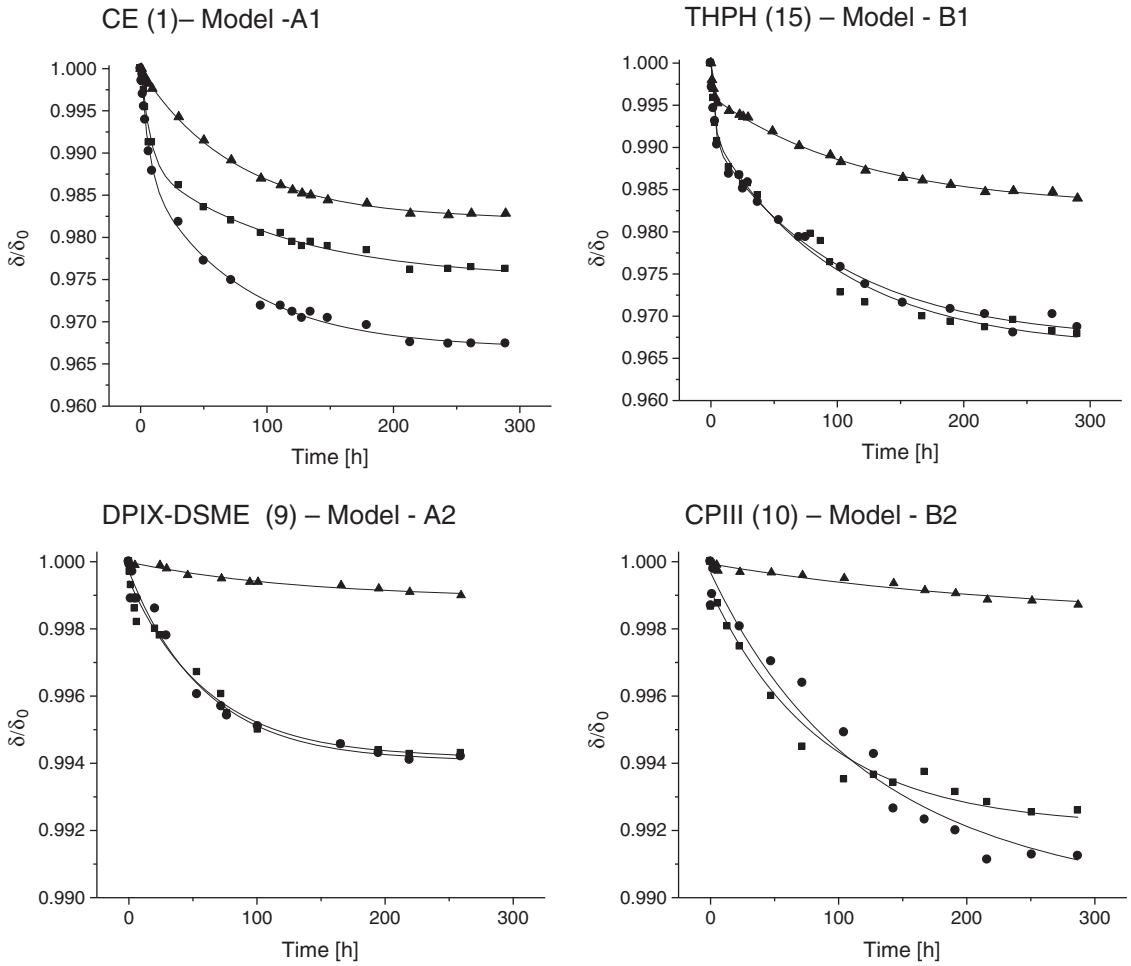

Fig. 6. Normalized chemical shift δ/δ_0 of DOPC inner (if split) or inner and outer (not split) choline -$N^+(CH_3)_3$ (triangle), -$(CH_2)_n$- (square), and ω-CH_3 (circle) resonances as function of time after addition of PS. Experiment conditions: PS/DOPC 0.1, pH 6.9. Solid lines correspond to fitting curves (fitting function: Exp. Section).

Table 2
Classification of PS according to the behavior of inner and outer choline resonances, following the schemes in Fig. 5.

PS		Type	PS		Type
CE	**(1)**	A-1	DPIX-DSME	**(9)**	A-2
RG7	**(2)**	A-1	CPIII	**(10)**	B-2
CEMED	**(3)**	A-1	DPIX-DS	**(11)**	B-2
m-CEMED	**(4)**	A-1	TCPhP	**(12)**	B-2
MACE	**(5)**	A-1	TSPhP	**(13)**	B-2
Arg-CE	**(6)**	A-1	TMPyP	**(14)**	B-2
Tyr-CE	**(7)**	A-1	THPhP	**(15)**	B-1
HPIX	**(8)**	A-2			

outer choline signal, initially overlapping with the inner choline signal, undergoes either the same (Model-B2) or a more pronounced (Model-B1) upfield shift evolution compared to the inner choline resonance, indicating a PS accumulation at the outer surface in both cases. Table 2 summarizes the classification of the investigated PSs with respect to these different time evolutions of the two choline resonances (for corresponding spectra of all remaining PSs, see supplemental Figure S7).

Within the applied concentration range, the classification is independent of the PS-concentration, i.e. the same trend was observed for low or high PS amounts.

In Fig. 6, plots of normalized chemical shifts δ/δ_0 of the three inner DOPC signals (inner choline —$N^+(CH_3)_3$, —$(CH_2)_n$— and ω-CH_3) versus time for four selected PS/DOPC systems, i.e. representatives of the four Models-A1, -A2, -B1, and -B2 are shown (for corresponding plots of all remaining PSs, see supplemental Figures 1S–6S). The δ/δ_0-values are probably best suited for giving an idea of PS diffusion and uptake.

Comparing the different temporal evolutions the following observations can be made: (i) during the observed time the normalized chemical shifts δ/δ_0 of all three resonances decrease indicating PS uptake into the membrane for all four models. (ii) The decrease typically follows a mono- or bi- exponential decay and reaches an equilibrium value after about ~300 h. (iii) δ/δ_0 equilibrium values of the three inner DOPC signals are different, indicating different amounts of PS uptake into and different PS distribution within the membrane.

Figs. 7 and 8 show the corresponding δ_e/δ_0 equilibrium values for Type-A and Type-B PSs. The final equilibrium values of δ_e/δ_0 for all PSs are very different: They are generally lower at high (0.1) than at low (0.025) PS/DOPC molar ratio and depend on the type and structure of the investigated PS. In particular at higher PS concentration, the normalized equilibrium values δ_e/δ_0 of all DOPC signals (—$(CH_2)_n$—, ω-CH_3 and —$N^+(CH_3)_3i$) are significantly lower in Model-A1 and -B1 (Fig. 7), as compared to Model-A2 and -B2 (Fig. 8), clearly indicating higher PS uptake into the lipophilic membrane bilayer.

Moreover δ_e/δ_0 values of the -$(CH_2)_n$- and ω-CH_3 resonances are lower in general for all four Models as compared to the inner choline -$N^+(CH_3)_3$ resonance which suggests higher PS concentration in the lipophilic membrane part as compared to the inner membrane surface. For some PSs (mainly Type-A1) the observed chemical shift changes were larger for the terminal ω-CH_3 than for the -$(CH_2)_n$- resonances. This suggests preferential location in the membrane centre. However, changes of the -$(CH_2)_n$- signal shift are more complex to explain because the signal encompasses both, lipid chain regions close to the head-group (C_4-C_7) and regions close to the membrane core (C_{12}-C_{17}).

The different behavior of the four porphyrin models can be interpreted on the basis of their different structural properties as outlined subsequently.

3.3.2. Model-A1 and -A2

The initial split of the choline signals observed in Model-A1 and -A2 indicates measureable initial anchoring in the outer surface for all Type-A PSs, which is attributed to their amphiphilic character (see Section 3.2.2). Accordingly, the initial split values (Fig. 5, Table 1) are on average larger for Type-A1 PSs with distinct amphiphilicity, than for Type-A2 PSs with less pronounced amphiphilicity. Even though this difference was not used to define the subclasses, it supports the classification into A1 and A2 derived from the temporal chemical shift changes. The downfield shift evolution of the outer choline signal observed in Model-A1 (Fig. 5) is attributed to PS depletion in the outer layer and may occur for several reasons: (i) PS diffusion from the outer to the inner layer is more prominent than the PS uptake process from the external phase into the outer layer and hence, penetration towards the inner layer is not sufficiently compensated, (ii) PS depletion in the external bulk is caused by slow PS self-aggregation reducing the availability of PS for further membrane uptake, (iii) the outer membrane surface is increasingly covered by PS aggregates blocking further penetration of PS monomers or (iv) the maximal PS uptake capacity is reached and the vesicles are PS saturated. Which of the above reasons applies is not yet clear and is subject to further investigations.

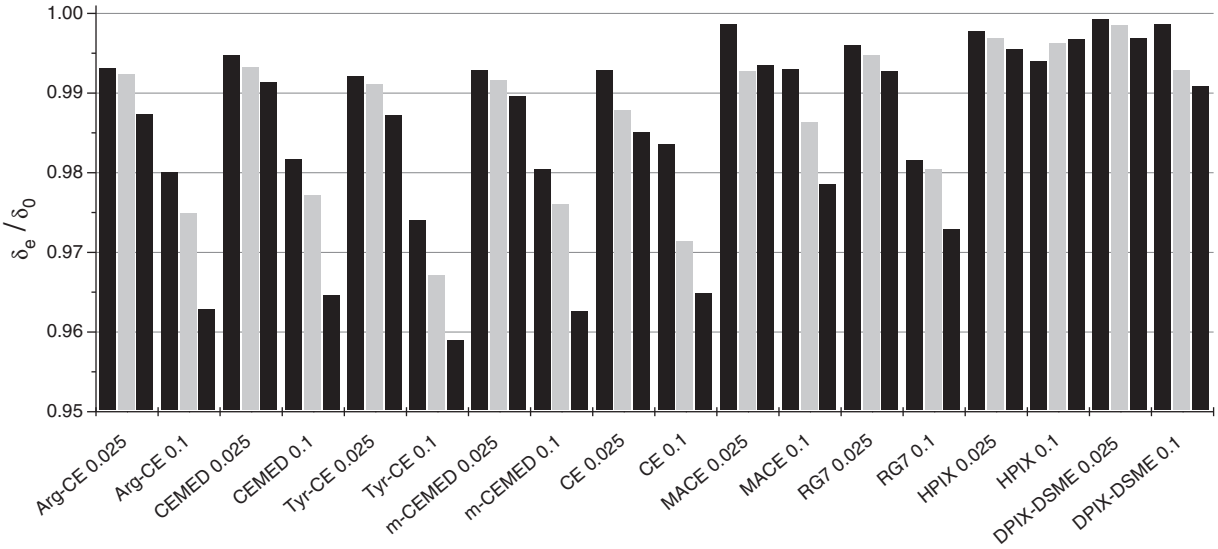

Fig. 7. Normalized chemical shift δ_e/δ_0 of DOPC inner choline —$N^+(CH_3)_3$ (black bar), —$(CH_2)_n$— (light gray bar), and ω-CH_3 (gray bar) resonances at equilibrium in the presence of Type-A PSs at low and high PS/DOPC molar ratio (0.025 and 0.1).

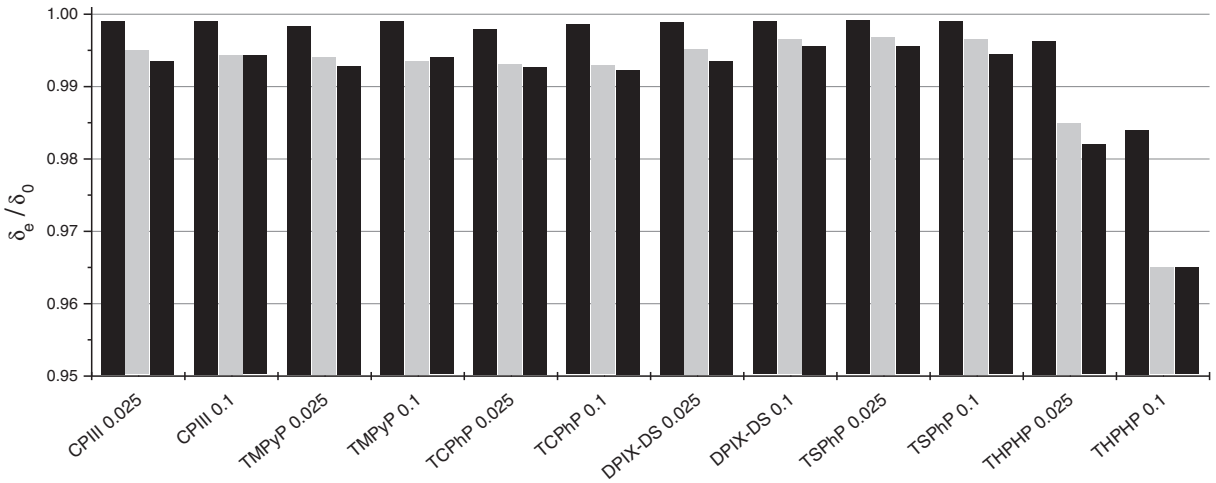

Fig. 8. Normalized chemical shift δ_e/δ_0 of DOPC inner choline —$N^+(CH_3)_3$ (black bar), —$(CH_2)_n$— (light grey bar), and ω-CH_3 (gray bar) resonances at equilibrium in the presence of Type-B PSs at low and high PS/DOPC molar ratio (0.025 and 0.1).

For Model-A2 the simultaneous upfield shifts of the inner and outer choline resonances (Fig. 5) indicate an increase of PS in both layers. However and in contrast to Model-A1 the uptake of PS from the external medium by the outer layer seems to be larger than the diffusion from the outer to the inner layer. This is corroborated by the higher equilibrium values δ_e/δ_0 of the inner PL signals suggesting lower PS uptake by the inner membrane for Type-A2 porpyhrins (Fig. 6).

Different PS uptake by the inner membrane layers may again be attributed to the porphyrins amphiphilicity.

As mentioned above, all Type-A PSs are amphiphilic, with different degrees of amphiphilicity for Type-A1 and Type-A2 respectively. Model-A1 PSs (compounds (1) through (7)) with two moieties of distinct hydrophilic and lipophilic character each are certainly more amphiphilic as compared to Type-A2 PSs (compounds (8) and (9)) with a less distinct lipophilic moiety. This is best demonstrated with the Type-A1 and -A2 representatives CE (1) and DPIX-DSME (9) respectively. CE (1) comprises a highly polar moiety with three carboxylic groups on one side and a highly unpolar moiety with no polar substituents on the other side. In contrast, for DPIX-DSME (9) the hydrophilic and lipophilic character in the two moieties are both attenuated due to the presence of two ester groups (instead of three carboxyl groups) and two sulfonic acid residues (instead of no polar substituents) respectively.

It is therefore reasonable to assume that higher PS uptake by the lipophilic membrane layers may be achieved for Type-A1 porphyrins with distinct lipophilic moieties as compared to the more polar Type-A2 porpyhrins with their higher affinity for the cationic choline groups in the outer surface.

These results are in agreement with other studies, where it has been demonstrated that amphiphilic properties of the PS played a crucial role in the interactions between PSs and membranes. [13,14] In particular it is important to note that not strictly amphiphilic PSs (as Type-A2) show a lower membrane uptake compared to the pure amphiphilic PSs (Type-A1). Similar conclusions, drawn from fluorescence studies, have been reported in the literature [15].

Additional structural properties such as different acidities of the lateral substituents and the pH dependent extent of deprotonation will certainly also play a role in the uptake process and may be responsible for minor differences among the representatives of a given PS Type. As an example, for MACE (5), a Type-A1 representative, δ_e/δ_0 values (Fig. 7) and the initial split of the choline signals were found to be greater than for the other Type-A1 PSs. This indicates enhanced surface anchoring and attenuated penetration and can be explained by the presence of four (instead of three for the other Type-A1 PSs) carboxylic groups. In combination with the distinct amphiphilicity of MACE, they are responsible for a strong electrostatic interaction with the outer membrane head groups and a high anchoring affinity as reflected by a high initial choline split value. However, this strong electrostatic interaction also attenuates the release of MACE into the bilayer as has been previously shown for this compound [23]. The increased polarity of its hydrophilic moiety decreases its affinity for the lipophilic membrane interior and consequently its membrane-diffusion and uptake.

To summarize, some of the Type-A1 PSs seem to have a major propensity to penetrate into the membrane layer (like compounds (1)-(4) and (6)-(7)). However, for both Type-A porphyrins penetration and trans-membrane distribution can be hindered if (i) the PS is retained in the outer layer due to strong electrostatic binding and decreased affinity for the lipophilic membrane core (like MACE (5) and DPIX-DSME (9)), or (ii) the initial surface affinity is low and only a little amount of PS resides in the outer layer at the beginning so that no significant concentration gradient is built up across the membrane (like HPIX (8) and DPIX-DSME (9)).

3.3.3. Model-B1 and -B2

For Type-B PSs no initial split of the choline signal is observed, indicating low or even no initial surface affinity. This is attributed to the missing or very weak amphiphilic properties of Type-B porphyrins (see section 3.2.3). Two different time evolutions were found for the choline signals (Fig. 5) with increasing splitting after initial signal broadening (Model-B1) and with no splitting (Model-B2) respectively. The slight upfield shifts observed for the inner and outer choline signals indicate PS residing near both the outer and inner surface and hence porphyrin uptake for both Type-B models. However, the amount near the outer and inner surface is different for Type-B1 PSs and seems equal for Type-B2 PSs respectively. Hence uptake of further PSs is clearly faster than diffusion across the bilayer for Type-B1 as opposed to Type-B2 PSs. This may be explained by the higher polarity of Type-B2 PSs with four highly polar and ionized carboxylic and sulfonic acid residues compared to Type-B1 PSs with less polar, non-ionizable groups. High polarity means higher affinity to the polar outer surface and low affinity to the lipophilic bilayer with low diffusion rates. Higher affinity for the hydrophobic membrane interior for the less polar Type-B1 porphyrin can be deduced from the δ_e/δ_0 equilibrium chemical shift values of the lipid chain resonances (Figs. 6 and 8).

These Type-B1 values are very similar to the corresponding values obtained for Type-A1 porphyrins despite their different structural properties. This similar behavior most probably results from the interdependence of the two main steps of membrane porphyrin

interaction. The second step (diffusion into the membrane) is dependent on the progress of the first step (anchoring in the outer surface) and therefore depends on both, the amphiphilicity and the lipophilicity of the porphyrin. Despite the low initial enrichment of Type-B1 PSs in the outer membrane surface, their diffusion into the membrane bilayer is large because of their high lipophilic affinity and hence diffusion is affinity driven. The less lipophilic Type-A1 PSs on the other hand with less membrane core affinity show similar membrane penetration because of their high initial enrichment in the outer membrane surface and hence diffusion is concentration driven. Even though, among the different PSs investigated in the current work, there is only one Type B1 representative, i.e. compound (15), its membrane interaction can be clearly distinguished from the other compounds as shown in Figs. 5 and 8 and therefore may justify forming a separate class. In particular, compound (15) is the only one with overall non-ionic/ionizable but intermediately polar substituents. Further investigations will need to be performed to prove the hypothesis that similar PS structures will likewise exhibit Type B1 behavior with respect to their membrane interaction.

The very low uptake of the Type-B2 PSs is demonstrated by the general high values of δ_e/δ_0 equilibrium chemical shift. These values are on average higher than for all the other PSs, demonstrating that Type-B2 PSs are the compounds that have less interaction with the membrane. These findings are in agreement with results published by others groups, where ionic and amphiphilic PSs were evaluated in terms of membrane affinity [35] and in terms of activity in photochemical gene transfection [13]. Both studies concluded that symmetric and ionic PSs have the lowest membrane affinity.

4. Conclusions

In the present study ^{1}H-NMR spectroscopy was used to investigate the interaction of a series of porphyrinic photosensitizers (PSs) with model membranes. NMR spectroscopy has proved to be a most potential tool for getting a close insight into the interaction. Taking advantage of several site specific membrane parameters such as chemical shifts, e.g. the choline ^{1}H signals of the inner and outer membrane surface, signal intensities and the time evolution of these signals, details of the PS-membrane interaction could be unraveled. The structural variety of the 15 investigated PSs allowed a relationship between the PS chemical structure and the type of interaction to be recognized. Four different types of interaction have been found, assigned as Model-A1, -A2, -B1 and -B2 respectively.

According to our experimental results the porphyrin-membrane interaction consists of two main steps: 1. The electrostatically driven first porphyrin adsorption to the amphiphilic outer membrane surface layer, fast on the NMR time scale 2. The slow penetration of the porphyrin into the non-polar membrane interior followed by diffusion and distribution within the lipophilic bilayer which can be monitored by NMR. The rate and extent of these two steps are mainly affected by two different porphyrin structural properties, amphiphilicity and overall polarity.

High and fast uptake into the outer surface, the first step of porphyrin-membrane interaction, could be observed for non-symmetrical, highly amphiphilic Type-A1 porphyrins, whereas medium surface affinity was observed for the less amphiphilic Type-A2 porphyrins. Low or even undetectable small initial uptake into the outer surface on the other hand occurs with the symmetrical non-polar (Type-B1) and polar (Type-B2) porphyrins.

In contrast and most interestingly, fast trans-membrane diffusion and high porphyrin uptake into the lipophilic membrane core, the second step of porphyrin-membrane interaction, is observed for Type-A1 and Type-B1 porphyrins, whereas Type-A2 and Type-B2 porphyrins show correspondingly slow diffusion and low uptake by the membrane interior.

Therefore, the first step of interaction seems to be influenced exclusively by the amphiphilicity of the porphyrin. The second step however seems to be governed by both, amphiphilicity and overall lipophilicity, two diverging structural properties. Thus, the progress of step two depends on the extent of step one as outlined below.

High penetration into the lipophilic membrane core is certainly facilitated by low porphyrin polarity (Type-B1). Since there is only low initial enrichment of this type of porphyrins in the amphiphilic outer membrane surface, the uptake into the membrane interior is obviously affinity driven in this case and remarkable loadings of the membrane interior are achieved despite low initial affinity.

However, high penetration into the lipophilic membrane interior occurs also with highly amphiphilic porphyrins (Type-A1). With high initial enrichment of this type of porphyrins in the amphiphilic outer membrane surface, the uptake into the membrane core is obviously concentration driven in this case and remarkable loadings of the membrane interior are achieved despite the enhanced polarity of this type of porphyrin.

On the other hand for symmetrical, non-amphiphilic and highly polar (Type-B2) porphyrins and non-symmetrical, amphiphilic, but highly polar (Type-A2) porphyrins membrane interior loadings are quite poor.

Nevertheless and when comparing the two structural properties, more important for PS uptake into the membrane bilayer is most probably the degree of lipophilicity instead of amphiphilicity. Obviously symmetric, highly lipophilic, but weakly amphiphilic PSs may overcome the outer surface barrier and accumulate in the membrane core. The size of the non-polar moiety of highly amphiphilic PSs is assumed to be large and lipophilic enough to reach sufficient affinity and hence similar high membrane loadings.

In summary, the NMR approach is a valuable method for studying the interactions between PSs and model membranes on a submolecular level. Relationships between porphyrin and membrane structural properties allow principles governing corresponding interactions to be deduced and recognized. These perceptions are useful for better predicting the subcellular distribution of a given porphyrin in a membrane and hence might contribute to improved drug design in the field of PDT.

Acknowledgments

Support was obtained from the Swiss National Science Foundation (SNF), grant # 200021–119691.

Appendix A. Supplementary data

Supplementary data to this article can be found online at doi:10.1016/j.bbamem.2011.02.011.

References

[1] D. Dolmans, D. Fukumura, R.K. Jain, Photodynamic therapy for cancer, Nat. Rev. Cancer 3 (2003) 380–387.
[2] M.R. Hamblin, P. Mroz, History of PDT: The First Hundred Years, Artech House, 2008.
[3] I.J. MacDonald, T.J. Dougherty, Basic principles of photodynamic therapy, J. Porphyrins Phthalocyanines 5 (2001) 105–129.
[4] A.E. O'Connor, W.M. Gallagher, A.T. Byrne, Porphyrin and nonporphyrin photosensitizers in oncology: preclinical and clinical advances in photodynamic therapy, Photochem. Photobiol. 85 (2009) 1053–1074.
[5] O.J. Norum, P.K. Selbo, A. Weyergang, K.E. Giercksky, K. Berg, Photochemical internalization (PCI) in cancer therapy: from bench towards bedside medicine, J. Photochem. Photobiol., B 96 (2009) 83–92.
[6] K. Berg, M. Folini, L. Prasmickaite, P.K. Selbo, A. Bonsted, B.O. Engesaeter, N. Zaffaroni, A. Weyergang, A. Dietze, G.M. Maelandsmo, E. Wagner, O.J. Norum, A. Hogset, Photochemical internalization: a new tool for drug delivery, Curr. Pharm. Biotechnol. 8 (2007) 362–372.
[7] A. Szurko, M. Rams, A. Sochanik, K. Sieron-Stoltny, A.M. Kozielec, F.P. Montforts, R. Wrzalik, A. Ratuszna, Spectroscopic and biological studies of a novel synthetic chlorin derivative with prospects for use in PDT, Bioorg. Med. Chem. 17 (2009) 8197–8205.

[8] V. Kral, J. Kralova, R. Kaplanek, T. Briza, P. Martasek, Where is prophyrin chemistry going? Physiol. Res. 55 (2006) S3–S26.
[9] C. Pavani, A.F. Uchoa, C.S. Oliveira, Y. Iamamoto, M.S. Baptista, Effect of zinc insertion and hydrophobicity on the membrane interactions and PDT activity of porphyrin photosensitizers, Photochem. Photobiol. Sci. 8 (2009) 233–240.
[10] S.P. Songca, B. Mbatha, Solubilization of meso-tetraphenylporphyrin photosensitizers by substitution with fluorine and with 2, 3-dihydroxy-1-propyloxy groups, J. Pharm. Pharmacol. 52 (2000) 1361–1367.
[11] W.M. Sharman, J.E. van Lier, A new procedure for the synthesis of water-soluble tricationic and -anionic phthalocyanines, J. Porphyrins Phthalocyanines 9 (2005) 651–658.
[12] M.J. Garland, C.M. Cassidy, D. Woolfson, R.F. Donnelly, Designing photosensitizers for photodynamic therapy: strategies, challenges and promising developments, Future Med. Chem. 1 (2009) 667–691.
[13] L. Prasmickaite, A. Høgset, K. Berg, Evaluation of different photosensitizers for use in photochemical gene transfection, Photochem. Photobiol. 73 (2001) 388–395.
[14] H. Mojzisova, S. Bonneau, P. Maillard, K. Berg, D. Brault, Photosensitizing properties of chlorins in solution and in membrane-mimicking systems, Photochem. Photobiol. Sci. 8 (2009) 778–787.
[15] F. Rancan, A. Wiehe, M. Nöbel, M.O. Senge, S. Al Omari, F. Böhm, M. John, B. Röder, Influence of substitutions on asymmetric dihydroxychlorins with regard to intracellular uptake, subcellular localization and photosensitization of Jurkat cells, J. Photochem. Photobiol., B 78 (2005) 17–28.
[16] S.A. Sibani, P.A. McCarron, A.D. Woolfson, R.F. Donnelly, Photosensitiser delivery for photodynamic therapy. Part 2: systemic carrier platforms, Expert Opin. Drug Deliv. 5 (2008) 1241–1254.
[17] M. Regehly, K. Greish, F. Rancan, H. Maeda, F. Bohm, B. Roeder, Water-soluble polymer conjugates of ZnPP for photodynamic tumor therapy, Bioconjug. Chem. 18 (2007) 494–499.
[18] F. Rancan, M. Helmreich, A. Molich, N. Jux, A. Hirsch, B. Roeder, F. Boehm, Intracellular uptake and phototoxicity of 3(1), 3(2)-didehydrophytochlorin-fullerene hexaadducts, Photochem. Photobiol. 83 (2007) 1330–1338.
[19] S. Bonneau, C. Vever-Bizet, Tetrapyrrole photosensitisers, determinants of subcellular localisation and mechanisms of photodynamic processes in therapeutic approaches, Expert Opin. Ther. Pat. 18 (2008) 1011–1025.
[20] V.P. Zorin, I.I. Khludeyev, T.E. Zorina, The distribution of porphyrin sensitizers among serum proteins and blood cells, Biofizika 45 (2000) 313–319.
[21] H. Mojzisova, S. Bonneau, C. Vever-Bizet, D. Brault, Cellular uptake and subcellular distribution of chlorin e6 as functions of pH and interactions with membranes and lipoproteins, Biochim. Biophys. Acta: Biomembr. 1768 (2007) 2748–2756.
[22] H. Mojzisova, S. Bonneau, C. Vever-Bizet, D. Brault, The pH-dependent distribution of the photosensitizer chlorin e6 among plasma proteins and membranes: a physico-chemical approach, Biochim. Biophys. Acta: Biomembr. 1768 (2007) 366–374.
[23] M. Vermathen, P. Vermathen, U. Simonis, P. Bigler, Time-dependent interactions of the two porphyrinic compounds chlorin e6 and mono-L-aspartyl-chlorin e6 with phospholipid vesicles probed by NMR spectroscopy, Langmuir 24 (2008) 12521–12533.
[24] M. Vermathen, M. Marzorati, P. Vermathen, P. Bigler, pH-dependent distribution of chlorin e6 derivatives across phospholipid bilayers probed by NMR spectroscopy, Langmuir 26 (2010) 11085–11094.
[25] D.J. Cabral, D.M. Small, H.S. Lilly, J.A. Hamilton, Transbilayer movement of bile-acids in model membranes, Biochemistry 26 (1987) 1801–1804.
[26] R.G. Males, F.G. Herring, A H-1-NMR study of the permeation of glycolic acid through phospholipid membranes, Biochim. Biophys. Acta: Biomembr. 1416 (1999) 333–338.
[27] C. Lagoueyte, G. Subra, P.A. Bonnet, J.P. Chapat, J.C. Debouzy, F. Fauvelle, F. Berleur, V. Roman, M. Fatome, J.P. Fernandez, Interaction and translocation of cysteamine (mercaptoethylamine) with model membranes: a N-15-NMR and H-1-NMR study, Eur. J. Pharm. Biopharm. 43 (1997) 73–81.
[28] Z.J. Wang, Y.Y. He, C.G. Huang, J.S. Huang, Y.C. Huang, J.Y. An, Y. Gu, L.J. Jiang, Pharmacokinetics, tissue distribution and photodynamic therapy efficacy of liposomal-delivered hypocrellin A, a potential photosensitizer for tumor therapy, Photochem. Photobiol. 70 (1999) 773–780.
[29] D. Rotin, P. Wan, S. Grinstein, I. Tannock, Cytotoxicity of compounds that interfere with the regulation of intracellular pH: a potential new class of anticancer drugs, Cancer Res. 47 (1987) 1497–1504.
[30] W.R. Light, J.S. Olson, Transmembrane movement of heme, J. Biol. Chem. 265 (1990) 15623–15631.
[31] M. Vermathen, E.A. Louie, A.B. Chodosh, S. Ried, U. Simonis, Interactions of water-insoluble tetraphenylporphyrins with micelles probed by UV-visible and NMR spectroscopy, Langmuir 16 (2000) 210–221.
[32] D. Uhríková, N. Kuçerka, A. Islamov, A. Kuklin, V. Gordeliy, P. Balgavý, Small-angle neutron scattering study of the lipid bilayer thickness in unilamellar dioleoylphosphatidylcholine vesicles prepared by the cholate dilution method: n-decane effect, Biochim. Biophys. Acta: Biomembr. 1611 (2003) 31–34.
[33] S.H. White, W.C. Wimley, Hydrophobic interactions of peptides with membrane interfaces, Biochim. Biophys. Acta: Biomembr. 1376 (1998) 339–352.
[34] N.C. Maiti, S. Mazumdar, N. Periasamy, Dynamics of porphyrin molecules in micelles. picosecond time-resolved fluorescence anisotropy studies, J. Phys. Chem. 99 (1995) 10708–10715.
[35] T.I. Rokitskaya, M. Block, Y.N. Antonenko, E.A. Kotova, P. Pohl, Photosensitizer binding to lipid bilayers as a precondition for the photoinactivation of membrane channels, Biophys. J. 78 (2000) 2572–2580.